Stator Line Current Spectrum Content of a Healthy Cage Rotor Induction Machine

Gojko Joksimović[1], Jakša Riger[1], Thomas Wolbank[2], Nedjeljko Perić[3], Mario Vašak[3]

Abstract – **The paper analyzes the stator current spectrum of a healthy squirrel cage induction machine. The knowledge of stator current spectrum of the healthy cage rotor induction machine is a starting point for diagnosis of different faulty regimes using a noninvasive diagnostic technique known as motor current signature analysis. Magnetomotive force (MMF) space harmonics, slot permeance harmonics as well as saturation of main magnetic flux path through the virtual air gap permeance variation are taken into analytical consideration. Air gap flux density waves were obtained by multiplying the corresponding MMF waves with air gap permeance waves. General rules which give the connection between the number of rotor bars and the existence of rotor slot harmonics in the stator current spectrum are derived, too. Their appearance as well as magnitude depends on the corresponding air gap flux density wave pole pair number. Predicted spectral components of the stator current are experimentally verified on two laboratory motors with different number of rotor bars.**

Index Terms – **Induction machine, Condition monitoring, Stator current spectrum, Slot harmonics, Saturation**

I. INTRODUCTION

On-line condition monitoring of electrical machines has become a very important issue in systems for protection of electric machines. Condition monitoring can significantly improve reliability and enable timely planning of repairs, particularly when it comes to high power machines i.e. high price machines or machines that are important from the system that includes them as prime mover point of view.

In order to monitor the machine's health condition and to make on-line diagnosis many different techniques have been developed. Among others, one can mention the measurement and spectral analysis of the axial magnetic flux by using the search coil, the vibration analysis techniques, stator current etc. [1].

Among the mentioned techniques motor current signature analysis (MCSA) has particularly significant importance. Stator line current frequency spectrum represents, a sort of speaking, an electrocardiogram of electrical machine. This technique is especially useful because it is non-invasive, and search coil is a machine stator winding itself, [2].

In order to make the correct interpretation of changes in the spectrum as a result of different faulty regimes, one should be familiar with current spectrum of the healthy machine, which is not an easy demand because of the complexity of electromagnetic processes, variable in space and time, which occur in the machine. In other words, it is necessary to have a powerful mathematical model that enables numerical modeling of the machine taking into account exact geometrical representation of the machine. On the other hand, in order to be able to interpret results from the numerical model on a proper manner it is necessary to have an appropriate analytical model. The most common approach for these purposes is MMF – permeance wave approach where resultant air gap magnetic flux density waves are a result of MMF and permeance wave multiplication [3].

Only the application of both models, numerical and analytical and with experimental verification, enables to draw exact conclusions about which spectral current component give sign of different faults in the machine.

It is common in literature that induction machine is modeled assuming infinitely high permeable magnetic core by which all analysis is reduced to the analysis of electromagnetic processes taking place in the air gap [4], [5]. This approach does not give a real picture of the stator current spectrum bearing in mind the fact that every induction machine is more or less saturated in rated operating mode.

This paper aims to analyze the stator current spectrum of healthy induction motor as a basis for analyzing the spectrum in different modes of failures. In first part of the

[1] Faculty of Electrical Engineering, University of Montenegro, Montenegro
[2] Faculty of Electrical Engineering, Vienna University of Technology, Austria
[3] Faculty of Electrical Engineering and Computing, University of Zagreb, Croatia

978-1-4244-9302-9/11/$26.00 ©2011 IEEE

paper a short reminiscence on the MMF space harmonics will be done. Second part of the paper deals with slot permeance harmonics, while in third part saturation of the main magnetic flux path in the machine is taken into account. Analytically predicted stator current spectral components are validated at the end of the paper through experimental spectra of two different machines.

II. SPACE MMF HARMONICS

Due to the three phase stator winding placement in the slots, the phase as well as the resultant rotating MMF wave shape is stepwise. Therefore, rotating MMF beside the fundamental harmonic with p pole pairs contain higher space harmonics. The aforementioned series of MMF space harmonics are defined by the well-known expression,

$$\nu = 6g + 1, \qquad g = 0, \pm 1, \pm 2, \ldots \tag{1}$$

where ν is harmonic order. Besides 5th and 7th space harmonics, which are a consequence of trapezoidal phase MMF shape, slot harmonics or more precisely, principal slot harmonics (PSH) are two of the most prominent higher space harmonics in the stepwise MMF waveform of the stator. Their existence is, in accordance with the definition of MMF, generated by the flow of current through the corresponding winding and a consequence of the discrete nature of the stator and rotor windings, i.e. their placement in the slots.

For a stator with S slots, in a motor with p pole pairs, stator slot harmonics are of order $\lambda S/p \pm 1$, $\lambda = 1,2,\ldots$ These harmonics belong to the series of the higher MMF space harmonics generated by a symmetrical three-phase stator winding supplied by a system of symmetrical three-phase voltages (1). In such a series they are, for $\lambda=1$, the most prominent space harmonics in the spectrum (known as PSH) and it is well known that these harmonics are not able to be attenuated using short pitched stator windings.

Rotor slot harmonics (RSH) are of much more interest in cage induction motors and RSH are not only the most prominent space harmonics of rotor MMF, but they also exist only in the spectrum beside the fundamental rotor MMF wave. Rotor cage reacts on the flux density waves from stator side with the following three series of MMF waves, [6],

$$M_1 = M_{1m}\cos\left(s_\nu \omega t - \nu p\theta_r\right), \tag{2}$$

$$M_2 = M_{2m}\cos\left(s_\nu \omega t + \left(\frac{\lambda R}{p} - \nu\right)p\theta_r\right), \tag{3}$$

$$M_3 = M_{3m}\cos\left(s_\nu \omega t - \left(\frac{\lambda R}{p} + \nu\right)p\theta_r\right), \tag{4}$$

where,

$$s_\nu = 1 - \nu(1 - s). \tag{5}$$

In an unsaturated machine these MMF waves interact with the constant air-gap permeance, producing the same shape of flux density waves. These waves, in the stator frame of reference, are:

$$B_1 = B_{1m}\cos\left(\omega t - \nu p\theta_s\right), \tag{6}$$

$$B_2 = B_{2m}\cos\left(\left(1 - \lambda\frac{R}{p}(1-s)\right)\omega t + \left(\frac{\lambda R}{p} - \nu\right)p\theta_s\right), \tag{7}$$

$$B_3 = B_{3m}\cos\left(\left(1 + \lambda\frac{R}{p}(1-s)\right)\omega t - \left(\frac{\lambda R}{p} + \nu\right)p\theta_s\right). \tag{8}$$

Therefore, all of the flux density space harmonics from stator side, rotor reflect at the fundamental frequency and a series of two additional slip dependent frequencies, located rather high in the stator current spectrum, that are known as the rotor slot harmonics, RSH, lower,

$$f_{RSH\_L} = \left(1 - \lambda\frac{R}{p}(1-s)\right)f_1, \tag{9}$$

and upper,

$$f_{RSH\_U} = \left(1 + \lambda\frac{R}{p}(1-s)\right)f_1, \tag{10}$$

where $\lambda=1,2,3\ldots$ For $\lambda=1$ one has the first order RSH or principal slot harmonics, PSH. These flux density waves, induce electromotive forces (EMFs) and lead to currents in the stator windings at the same frequencies.

It is known that the current components at RSH given by frequencies (4) and (5) are dependent on the rotor speed i.e. motor load. That is what makes them interesting and is the reason why these harmonics have found wide application in the sensorless speed estimation of induction motor drives using numerous different techniques for digital signal processing [7].

However, the existence of stator current components at frequencies given by (9) and (10) depends on the number of pole pairs in the flux density waves (7) and (8). In order that spectral component at the lower PSH frequency (9) exist in the stator current spectrum it is required that the number of pole pairs in the flux density wave (7) is equal to the number of pole pairs produced by the stator winding, or, in other words, $R/p-\nu$ for some value of ν must belong to the group $\mathbf{H}=(6k+1)$. It further means that:

$$R_{L\_PSH} = p[6(g+k)+2],\ g = 0,\pm1,\pm2,\ldots;\ k = 0,\pm1,\pm2,\ldots \tag{11}$$

It can be easily concluded from (11) that for a rotor with R bars, in a p pole pair motor,

$$R_{L\_PSH} = (6n+2)p, \qquad n = 0, 1, 2, 3, ... \tag{12}$$

only lower PSH in the stator current spectrum will exist (R_{L_PSH}=4, 16, 28, 40, ...in a four pole motor). On the other hand, the condition for the existence of the upper PSH is satisfied for rotors with following number of bars,

$$R_{U\_PSH} = -p[6(g+k)+2], \; g = 0, \pm1, \pm2, .. \, k = 0, \pm1, \pm2, \tag{13}$$

which is equivalent to the following,

$$R_{U\_PSH} = (6n-2)p, \qquad n = 1, 2, 3, ... \tag{14}$$

i.e. R_{U_PSH}=8, 20, 32, 44, ...in a four pole motor.

In order that both of these PSH's exists in the stator current spectrum, the number of rotor bars in p pole pairs motor, must be the mean value of (12) and (14),

$$R_{BOTH\_PSH} = 6np, \qquad n = 1, 2, 3... \tag{15}$$

which is identical with the "forbidden" combinations of stator and rotor slot numbers, [8], (R_{BOTH_PSH}=12, 24, 36, 48, ...in a four pole motor). Rotors with R bars in p pole pair motor, which do not satisfy any of the conditions (12), (14) and (15), will not have any PSHs in the stator current spectrum, under symmetrical stator windings and symmetrical voltage supply conditions.

III. SLOT PERMEANCE HARMONICS

Besides the MMF space harmonics in the stator or rotor MMF wave that have been described, another effect exists in a real induction motor which generates EMFs and currents in stator windings at the same frequencies given by (9) and (10), as it will be explained below. This is the stator and rotor slotting effect i.e. the air gap length that varies with both space and time as a function of rotation of the rotor. As was stated previously, both space slot harmonics and slot permeance harmonics induce EMFs and lead to currents at the same frequencies. Hence, the distinction between the contributions of these components is blurred. The main differentiation between these two effects is that rotor MMF space harmonics exist only in case when current flows through the cage winding, even in the no-load case. This is as a consequence of high frequency rotor currents induced by rotating flux density wave harmonics from the stator side. For the existence of rotor permeance slot harmonics this precondition is not needed. Even a slotted rotor without any winding, rotating in the motor by some external means e.g an auxiliary motor, will lead to stator windings current components at frequencies given by (9) and (10) if the stator winding is connected to the voltage supply. In this case, the slip in (9) and (10) is simply the difference between the synchronous speed and the speed of the auxiliary motor. The reason for the existence of these stator current components is that the self inductance of the stator windings becomes a function of time as a consequence of variable permeance due to the rotor rotation.

The real induction motor air gap permeance is variable in both space and time as a consequence of stator and rotor slotting and their mutual position as a function of rotor rotation. Taking into account only the fundamental harmonic of air gap permeance series, the air gap permeance function is commonly described by following series, [9]-[11],

$$P(\theta_s, \theta_r) = \frac{1}{g} + k_s \cos(S\theta_s) + k_r \cos(R\theta_r) + k_{sr} \cos(S\theta_s - R\theta_r) + ... \tag{16}$$

where coefficients k_s, k_r, k_{sr} depends on the geometrical dimensions of the air gap and stator and rotor slot mouth width. Now, consider the situation when stator MMF waves given by,

$$M_{sv}(t, \theta_s) = M_{sv\max} \cos(\omega t - \nu p \theta_s), \tag{17}$$

act on the third term of (16). As a result, two flux density waves are obtained, expressed in the stator frame of reference as,

$$B_{sv1}(t, \theta_s) = B_{sv1\max} \cos\left(\left(1 - \frac{R}{p}(1-s)\right)\omega t + \left(\frac{R}{p} - \nu\right)p\theta_s\right), \tag{18}$$

$$B_{sv2}(t, \theta_s) = B_{sv2\max} \cos\left(\left(1 + \frac{R}{p}(1-s)\right)\omega t - \left(\frac{R}{p} + \nu\right)p\theta_s\right), \tag{19}$$

which are identical with waves (7) and (8).

On the other side, stator MMF waves (17) acting on the fourth term in the permeance expression (16), give flux density waves of the same frequencies but with different numbers of pole pairs given by:

$$B_{sv3}(t, \theta_s) = B_{sv3\max} \cos\left(\left(1 - \frac{R}{p}(1-s)\right)\omega t - \left(\frac{S-R}{p} + \nu\right)p\theta_s\right), \tag{20}$$

$$B_{sv4}(t, \theta_s) = B_{sv4\max} \cos\left(\left(1 + \frac{R}{p}(1-s)\right)\omega t + \left(\frac{S-R}{p} - \nu\right)p\theta_s\right). \tag{21}$$

As will be shown, this difference in pole pair number could have, at certain combination of stator, rotor slot and pole pair number, a significant influence on stator current components amplitudes at these frequencies.

IV. SATURATION PERMEANCE HARMONICS

Saturation of the main magnetic flux path in a machine can be modeled by making the air-gap length a function of

the saturation level and spatial position, Fig 1. In this approach maximum value of the virtual air-gap length corresponds to the maxima/minima of the main magnetic flux density wave, while the minimum value of the virtual air-gap length (equal to the effective value of the air-gap length) corresponds to the zero value of the main magnetic flux density wave.

Accordingly, the air-gap permeance function, neglecting the stator and rotor slotting, is described with the following expression, [12]-[14],

$$P(\theta_s,\beta)=\frac{1}{g_0}-k_m-k_m\cos(2p\theta_s-2\beta), \tag{22}$$

where g_0 is the effective air-gap length and p is the machine's number of pole pairs.

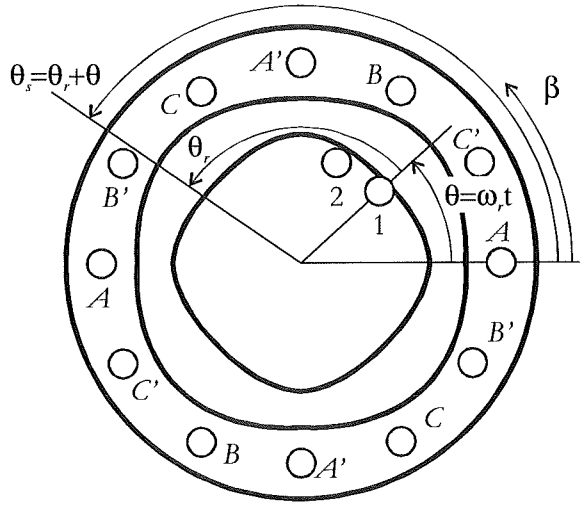

Fig 1. Virtual air-gap length variation along the machine circumference due to the main magnetic flux path saturation, p=2, β=π/2 rad.

Angle θ_s (in mechanical radians) defines position along the stator circumference, while β (in electrical radians) describes the angular position of the air-gap flux density maximum in the stator frame of reference. The factor k_m is correlated with the saturation factor in the following manner. Product of the permeance function and the fundamental MMF wave $M_{1\max}\cos(\omega t-p\theta_s)$ gives two flux density waves:

$$B(t,\theta_s)=M_{1\max}\left(\frac{1}{g_0}-\frac{3}{2}k_m\right)\cos(\omega t-p\theta_s)-M_{1\max}\frac{k_m}{2}\cos(3\omega t-3p\theta_s). \tag{23}$$

Maximum value of the fundamental flux density wave in (23) should correspond to the saturated condition of the machine (B_{sat} ~E_{sat}~U_{sat}). In unsaturated machine, maximal value of the fundamental flux density wave (B_{nonsat}~E_{nonsat}~U_{nonsat}) should correspond to the inverse value of the effective air-gap length, i.e.:

$$\frac{1}{g_0}:U_{non\_sat}=\left(\frac{1}{g_0}-\frac{3}{2}k_m\right):U_{sat}. \tag{24}$$

As the saturation factor is the ratio of the fundamental components of the air-gap voltage in unsaturated and saturated conditions,

$$k_{sat}=\frac{U_{non\_sat}}{U_{sat}}, \tag{25}$$

previous relationship results in:

$$k_m=\frac{2}{3}\frac{1}{g_0}\frac{k_{sat}-1}{k_{sat}}. \tag{26}$$

The air-gap permeance function (22) now attains a compact form,

$$P=P_1+P_2=P_1+P_{2m}\cos(2p\theta_s-2\beta), \tag{27}$$

where,

$$P_1=\frac{1}{g_0}\left(1-\frac{2}{3}\frac{k_{sat}-1}{k_{sat}}\right), \tag{28}$$

$$P_{2m}=-\frac{2}{3}\frac{1}{g_0}\frac{k_{sat}-1}{k_{sat}}. \tag{29}$$

Symmetrical three-phase stator winding produces a series of MMF waves, described by the well-known relation,

$$M_s=M_{sm}\cos(\omega t-\nu p\theta_s) \tag{30}$$

where ν=6g+1, g=0,±1,±2,... These waves, in interaction with the air-gap permeance function (27) produce a myriad of magnetic flux density waves. It should be noted that in a steady state condition β=ωt.

In a saturated machine, two different effects can be recognized. Firstly, rotor MMF waves (2)-(4) experience a variable air-gap permeance. In interaction with P_2 (27), rotor MMF waves produce the following flux density waves, in stator reference frame,

$$B_{11sat}=B_{11msat}\cos(\omega t+(\nu-2)p\theta_s), \tag{31}$$

$$B_{12sat}=B_{12msat}\cos(3\omega t-(\nu+2)p\theta_s), \tag{32}$$

$$B_{21sat}=B_{21msat}\cos\left(\left(1+\lambda\frac{R}{p}(1-s)\right)\omega t-\left(\frac{\lambda R}{p}-(\nu-2)\right)p\theta_s\right), \tag{33}$$

$$B_{22sat}=B_{22msat}\cos\left(\left(3-\lambda\frac{R}{p}(1-s)\right)\omega t+\left(\frac{\lambda R}{p}-(\nu+2)\right)p\theta_s\right), \tag{34}$$

$$B_{31sat}=B_{31msat}\cos\left(\left(1-\lambda\frac{R}{p}(1-s)\right)\omega t+\left(\frac{\lambda R}{p}+(\nu-2)\right)p\theta_s\right), \tag{35}$$

$$B_{32sat} = B_{32msat}\cos\left(\left(3+\lambda\frac{R}{p}(1-s)\right)\omega t-\left(\frac{\lambda R}{p}+(\nu+2)\right)p\theta_s\right). \quad (36)$$

As the pole pair number in (32) is a multiple of three for any ν, the third harmonic component in stator current spectrum cannot arise in a symmetrical machine connected to balanced three phase voltages.

Secondly, stator MMF waves in a saturated induction machine, through variable air-gap permeance $P_{2\theta}$, induce flux density waves that do not exist in an unsaturated machine. These waves are,

$$B_4 = B_{4m}\cos((1-(2-\nu)(1-s))\omega t+(\nu-2)p\theta_r), \quad (37)$$

$$B_5 = B_{5m}\cos((3-(\nu+2)(1-s))\omega t-(\nu+2)p\theta_r). \quad (38)$$

Due to these waves, new MMF waves in the cage rotor can appear. However, these new MMF waves, in the previously described manner, can induce the EMFs and lead to currents in the stator winding only at the same frequencies as in (31)-(36). Hence, in a saturated induction machine new stator current components can be expected only at the following frequencies: saturation lower,

$$f_{S\_L} = \left(3-\lambda\frac{R}{p}(1-s)\right)f_1, \quad (39)$$

and saturation upper harmonic:

$$f_{S\_U} = \left(3+\lambda\frac{R}{p}(1-s)\right)f_1. \quad (40)$$

Similarly as for the PSHs, in order that stator current components arise at frequencies given by (39), number of the pole pairs of the magnetic flux density waves (34) must be the same as the number of pole pairs that the stator winding itself produces. This means that, in order that stator current component at the lower saturation related frequency exists, $R/p-(\nu+2)$ must belong to group $\mathbf{H}=(6k+1)$ where k=0,±1, ±2, The same condition holds for the upper saturation related PSH.

V. STATOR CURRENT SPECTRUM CONTENT

Analytically predicted stator line current frequency components one can easily find in a spectrum of a real cage rotor induction motor. Measurements were conducted on two laboratory motors, with two different number of rotor bars. The stator current spectrum was recorded using a current clamp together with PicoScope® acquisition system.

A) *S*=36, *R*=28, *p*=2

Fig 2 shows experimentally obtained stator current spectrum for an induction motor with *S*=36 stator slots, *R*=28 rotor bars and *p*=2 pair of poles. In accordance with predictions, (12), only lower PSH exists in the spectrum at 616Hz, for *s*=4.86%. Additionally, both saturation related current components appear in the spectrum at predicted frequencies, (39), (40), i.e. at 516Hz and 816Hz for *s*=4.86%.

Moreover, saturation related component at 816Hz is one of the most prominent harmonics in the spectrum. This phenomenon could be easily explained by the following two facts: a) magnetic flux density wave (36) has fundamental number of pole pairs, *p*=2 for ν=−17; b) stator MMF space harmonic for ν=−17 is rather high because this harmonic is the stator slot harmonic (*S*=36, *p*=2). So, these two facts cumulatively lead to rather high current component at upper saturation-related frequency.

Other saturation-related current component at 516Hz is not so prominent because magnetic flux density wave (34) could have fundamental number of pole pairs only for ν=13, i.e. for stator MMF space harmonic of rather small magnitude.

Fig 2 shows, beside predicted, also additional current components. On a first place that are components at 150Hz, 250Hz and 350Hz. Third time harmonic in a stator current spectrum is a consequence of asymmetrical voltage supply, i.e. of some amount of inverse rotating magnetic flux wave in the air gap, ν=−1 in (32). Namely, none of the three-phase voltage supplies is ideally symmetrical as it is the case with real induction machine windings, too. The existence of 5th and 7th current time harmonic is due to the voltage time harmonics in three-phase supply voltages.

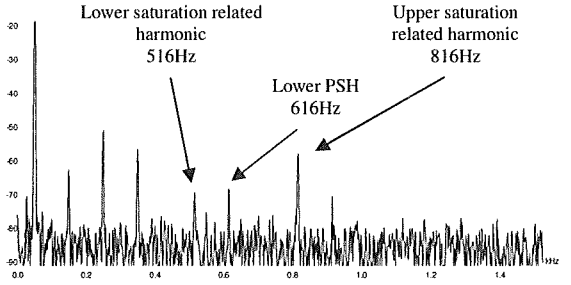

Fig 2. Experimentally recorded stator line current spectrum for loaded cage rotor induction motor with *S*=36 slots, *R*=28 bars and *p*=2 pole pairs. Slip *s*=4.86%.

B) *S*=36, *R*=32, *p*=2

Fig 3 shows record of stator current spectrum for loaded four pole cage rotor induction motor with *S*=36 stator slots and *R*=32 rotor bars @ *s*=6.4%. Only upper PSH exist in the spectrum according to (14). Moreover, upper PSH at 798Hz

is one of the most prominent higher harmonics in the whole stator current spectrum. Although the fundamental rotor current of the loaded motor has a significant influence on the PSH intensity, such a high PSH component can be explained only by the significant additional influence of slot permeance harmonics.

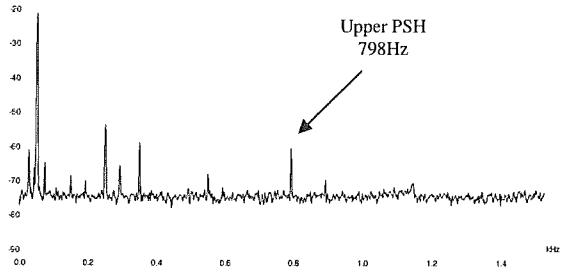

Fig 3. Experimentally recorded stator line current spectrum for loaded cage rotor induction motor with S=36 slots, R=32 bars and p=2 pole pairs. Slip s=6.4%.

Indeed, this motor has a number of stator and rotor slots such that the slot permeance harmonics will also have a very significant influence on the same PSH amplitude. From (21), it follows that $(S-R)/p-v=(36-32)/2-1=1$ and this means that the fundamental stator MMF wave through the slot permeance produces upper PSH. Hence, it might reasonably be expected that this upper principal slot harmonic is very prominent in the stator current spectrum in no-load, too. This explanation can be underpinned by stator current spectrum in no-load condition, Fig 4.

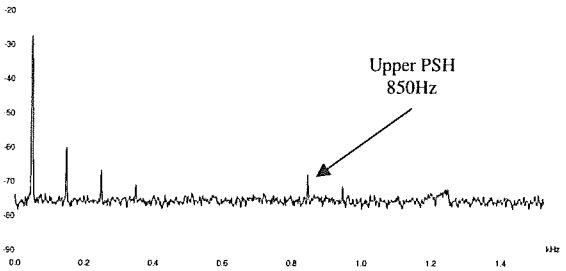

Fig 4. Experimentally recorded stator line current spectrum for unloaded (s=0) cage rotor induction motor with S=36 slots, R=32 bars and p=2 pole pairs

VI. CONCLUSIONS

Stator current spectrum content of healthy squirrel cage induction machine is analyzed. This is a starting point for diagnosis of any faulty regime of the machine by motor current signature analysis. MMF space harmonics, slot permeance harmonics as well as saturation of main magnetic flux path through the virtual air gap permeance variation are taken into analytical considerations. Air gap flux density waves are obtained by multiplying the corresponding MMF waves with air gap permeance waves. General rules which give the connection between the number of rotor bars and the existence of rotor slot harmonics in the stator current spectrum are derived, too. The predicted stator current spectrum content is experimentally verified on a two laboratory motors with different number of rotor bars.

ACKNOWLEDGMENT

The work to this paper was supported by the European Union in the SEE-ERA.NET PLUS framework as well as by the Ministry of Science - Montenegro.

REFERENCES

[1] W.T.Thomson, "A Review of On-Line Condition Monitoring Techniques for Three-Phase Squirrel-Cage Induction Motors – Past Present and Future", SDEMPED, September 1999, pp.3-18, Spain.

[2] W.T.Thomson, M.Fenger, "Current Signature Analysis to Detect Induction Motor Faults", *IEEE Industry Application Magazine*, July/August 2001.

[3] S.Nandi, S.Ahmed, H.A.Toliyat, "Detection of rotor slot and other eccentricity related harmonics in a three phase induction motor with different rotor cages," *IEEE Transactions on Energy Conversion*, Vol.16, No.3, pp. 253–260, September 2001.

[4] H.A.Toliyat, N.Al-Nuaim, "Simulation and Detection of Dynamic Air-Gap Eccentricity in Salient Pole Synchronous Machines," *IEEE Transactions on Industry Applications*, Vol.35, No.1, pp.86-93, 1999.

[5] G.M.Joksimović, "Dynamic Simulation of Cage Induction Machine with Air Gap Eccentricity," *IEE Electrical Power Applications*, Vol.152, No.4, pp.803-811, 2005.

[6] G.Joksimović, M.Đurović, J.Penman, "Cage Rotor MMF - Winding Function Approach", *IEEE Power Engineering Review Letters*, Vol.21, No.4, pp.64-66, April 2001.

[7] K.D.Hurst, T.G.Habetler, "A comparison of spectrum estimation techniques for sensorless speed detection in induction machines," *IEEE Trans. on Industry Applications*, Vol. 33, No.4, pp. 898-905, Jul/Aug 1997.

[8] T.Jokinen, V.Hrabovcova, *Design of rotating electrical machines*, John Wiley and Sons, 2009.

[9] S. Williamson, Y.N. Feng, "Slot-harmonic fields in closed-slot machines," *IEEE Trans. on Industry Applications*, vol. 44, No.4, pp.1165-1171, July/August 2008.

[10] S.Nandi, "Modeling of induction machines including stator and rotor slot effects," *IEEE Trans. on Industry Applications*, vol. 40, pp.1058-1065, July/August 2004.

[11] R.N.Andriamalala, H.Razik, L.Baghli, F.M.Sargos, "Eccentricity Fault Daignosis of a Dual-Stator Winding Induction Machine Drive Considering the Slotting Effects", *IEEE Transactions on Industrial Electronics*, vol.55, No.12, pp.4238-4251, December 2008.

[12] J.C.Moreira, T.A.Lipo, "Modeling of Saturated AC Machines Including Air Gap Flux Harmonic Components," *IEEE Transactions on Industry Applications*, Vol.28, No.2, pp.343-349, 1992.

[13] S.Nandy, "A detailed model of induction machines with saturation extendable for fault analysis", *IEEE Transactions on Industry Applications*, Vol.40, No.5, pp.1302-1309, 2004.

[14] G.Joksimović, "Line current spectrum analysis in saturated three-phase cage induction machine," *Electrical Engineering*, Springer Verlag, Vol.91, No.8, pp.425-437, April 2010.